

SiamAPN++: Siamese Attentional Aggregation Network for Real-Time UAV Tracking

Ziang Cao¹, Changhong Fu^{2,*}, Junjie Ye², Bowen Li², and Yiming Li³

Abstract— Recently, the Siamese-based method has stood out from multitudinous tracking methods owing to its state-of-the-art (SOTA) performance. Nevertheless, due to various special challenges in UAV tracking, *e.g.*, severe occlusion, and fast motion, most existing Siamese-based trackers hardly combine superior performance with high efficiency. To this concern, in this paper, a novel attentional Siamese tracker (SiamAPN++) is proposed for real-time UAV tracking. By virtue of the attention mechanism, the attentional aggregation network (AAN) is conducted with self-AAN and cross-AAN, raising the expression ability of features eventually. The former AAN aggregates and models the self-semantic interdependencies of the single feature map via spatial and channel dimensions. The latter aims to aggregate the cross-interdependencies of different semantic features including the location information of anchors. In addition, the dual features version of the anchor proposal network is proposed to raise the robustness of proposing anchors, increasing the perception ability to objects with various scales. Experiments on two well-known authoritative benchmarks are conducted, where SiamAPN++ outperforms its baseline SiamAPN and other SOTA trackers. Besides, real-world tests onboard a typical embedded platform demonstrate that SiamAPN++ achieves promising tracking results with real-time speed.

I. INTRODUCTION

Visual object tracking is a fundamental and challenging task, whose purpose is to track the indicated object frame by frame. By virtue of the powerful flexibility of unmanned aerial vehicles (UAVs), UAV tracking has drawn considerable attention such as aerial cinematography [1], path planning [2], and maneuvering targets tracking [3]. Despite numerous efforts, designing an efficient, accurate, and robust tracker for UAV remains an extremely challenging task due to the limited computational resources onboard the embedded platform. Meantime, the UAV tracking also suffers from various special challenges brought by the mobile platform, *e.g.*, fast motion, low resolution, severe occlusion, and long-term tracking.

Generally, there are two mainstream methods in the field of UAV tracking, *i.e.*, correlation filter-based (CF-based) and deep learning-based (DL-based) methods. In literature, online CF-based trackers are widely adopted due to their low computational complexity [4], [5]. Despite high efficiency, the accuracy and robustness of CF-based trackers hardly meet

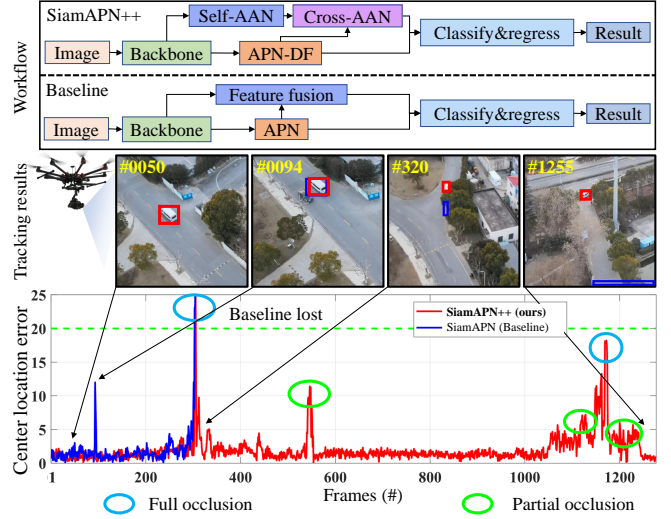


Fig. 1. Comparison between the baseline tracker and the proposed tracker, *i.e.*, SiamAPN and SiamAPN++. The figures from the top to bottom are workflow, tracking result, and center location error comparison. When facing the constantly occluded object, the AAN can emphasize and aggregate the effective information selectively, avoiding interference brought by the environment.

the requirement of UAV tracking in complex scenes. While the DL-based method has achieved significant advancement in terms of tracking performance by exploiting the deep features. Consequently, an efficient DL-based structure is a promising approach to balance performance and speed.

Among the DL-based trackers, the Siamese-based trackers enjoy their superiority due to their high potential in object tracking. The Siamese network structure is proposed by SiamFC [6], tracking by computing the similarity between template patch and search patch. Then, the anchor-based method was proposed in SiamRPN [7]. By introducing the region proposal network (RPN), it can obtain accurate bounding boxes. Based on RPN, further researches have been made to improve the tracking performance [8]–[10]. Since those anchors are pre-defined, the performance of anchor-based trackers is seriously influenced by the hyper-parameters associated with anchors. Besides, introducing pre-defined anchors without prior knowledge also impedes the tracking performance. To improve the generalization of trackers, the anchor-free method is proposed, which generally predicts the offset between ground truth and center point [11], [12]. Although the anchor-free method avoids the hyper-parameters, the phenomenon of imbalanced samples is still not properly solved.

The attention mechanism has also drawn much attraction

*Corresponding Author

¹Ziang Cao is with the School of Automotive Studies, Tongji University, 201804 Shanghai, China.

²Changhong Fu, Junjie Ye, and Bowen Li are with the School of Mechanical Engineering, Tongji University, 201804 Shanghai, China. changhongfu@tongji.edu.cn

³Yiming Li is with the Tandon School of Engineering, New York University, NY 11201 New York, United States.

in object tracking [10], [13]. However, the relationship and interdependencies of different features are neglected, impeding the robustness under various conditions. In this paper, a novel attentional Siamese tracker namely SiamAPN++ is proposed for real-time UAV tracking, mainly consisting of the attentional aggregation network (AAN) and anchor proposal network based on dual features (APN-DF) illustrated in Fig. 1. The AAN is divided into two subnetworks, *i.e.*, self-AAN and cross-AAN. The former aims to model the self-semantic interdependencies between the single feature map via spatial and channel dimensions while the latter focuses on emphasizing the interdependent channels of different feature maps and then aggregating them adaptively. Since the location information of anchors contains the semantic information of the object, it is integrated into the final features for robust and accurate tracking. Besides, to promote the robustness of tracking objects with various scales, dual features are introduced via general cross-AAN. By exploiting the interdependencies of features from different levels, APN-DF can generate more appropriate anchors than before. Real-world tests onboard the embedded platform shown in Fig. 1 prove the superior accuracy and robustness of SiamAPN++ while keeping a comparable speed to SiamAPN.

The main contributions of this work can be summarized as follows:

- A novel AAN is introduced to aggregate the self-semantic interdependencies of the single feature map via two methods and the cross-interdependence from different networks adaptively.
- The general cross-AAN is also adopted in APN-DF, improving the anti-interference and robustness of proposing anchors when facing objects with various scales.
- Extensive evaluations on two challenging UAV tracking benchmarks prove the superior performance of SiamAPN++ especially in fast motion, low resolution, severe occlusion. In addition, real-world tests conducted onboard the embedded platform strongly demonstrate impressive practicability and performance with real-time speed.

II. RELATED WORKS

Previously, CF-based trackers have been utilized widely on object tracking after MOSSE [14]. Depending on the high efficiency and expansibility, CF-based trackers can be deployed directly on UAVs. There is no doubt that the CF-based approach promoted the development of UAV tracking with satisfying speed [5], [15], [16]. However, the online tracking strategy hinders inevitably the structure of trackers, hardly learning and exploiting deeper features.

The Siamese-based network shows its huge potential in the domain of object tracking. SINT [17] firstly viewed the tracking task as matching the patch problem. Until the appearance of SiamFC [6], the advantage of the Siamese network is exposed. It aimed to measure the similarity between template and search path by employing a fully-convolutional neural network. Then, SiamRPN [18] introduced the RPN into the Siamese framework, viewing the tracking task as

classification and regression. DaSiamRPN [9] proposes a novel training method, improving the tracking performance. SiamRPN++ [8] and SiamDW [19] made it possible to utilize deeper networks. Despite obtaining state-of-the-art (SOTA) performance, those anchor-based trackers above suffer from hyper-parameters and imbalanced samples. In order to eliminate the problems, anchor-free trackers are proposed, *e.g.*, SiamFC++ [11], SiamCAR [12]. By redesigning the regression, the generalization of the trackers is raised. However, the influence caused by imbalanced samples is still existing. SiamAPN [20] brings a novel approach to handle the two problems at the same time, *i.e.*, proposing adaptive anchors. It increases the proportion of positive samples while adopting the no-prior structure of the anchor proposal network (APN).

In recent, much attention has been paid to the attention mechanism in many fields. The spactime non-local block is proposed in [21] for capturing long-range dependencies in the field of object detection, segmentation and pose estimation. DANet [22] developed the self-attention mechanism to address the scene segmentation task. In visual tracking, RASNet [13] adopted three attention branches to adapt the model without updating the model online in visual tracking. SiamAttn [10] exploits the attention mechanism module for providing an implicit manner to update the template. Besides, ECA-Net [23] proposes an efficient channel attention method for the deep convolutional neural network. However, those methods mentioned above merely focus on the self-attention or the relationship between template and search, neglecting the cross-interdependence between different level features.

In this work, the cross-AAN is proposed for exploring the potential of the cross-semantic interdependencies contained in different level features. Plus the self-interdependencies of the single feature map, the AAN can raise the expression ability of features significantly for handling the special challenges in UAV tracking. Besides, the APN based on dual feature structure is reconstructed for raising the anti-interference and robustness of proposing anchors and provide the reliable internal feature for AAN.

III. METHODOLOGY

A. Revisit SiamAPN

In this section, our baseline is revisited in brief, consisting of four networks, *i.e.*, feature extraction network, APN, feature fusion network, and classification®ression network. Different from pre-defined anchors, the APN adopts a single feature map to generate anchors, avoiding the hyper-parameters associated with anchors. Besides, it also decreases the number of negative samples, alleviating the phenomenon of imbalanced samples.

Although SiamAPN has achieved competitive performance, it remains two shortcomings: *a*) the performance is influenced easily by similar semantic information compared with variable appearance. *b*) the APN based on the single feature hardly maintains satisfying robustness when facing objects with various scales.

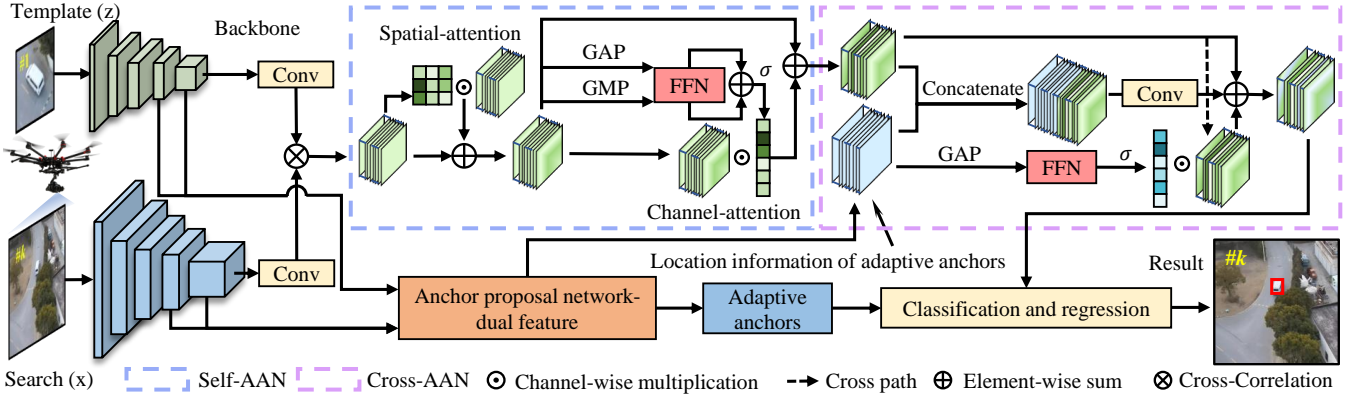


Fig. 2. The overview of the SiamAPN++ tracker. It composes of four subnetworks, *i.e.*, feature extraction network (backbone), classification and regression network, anchor proposal network-dual feature (APN-DF), and attentional aggregation network (AAN). (Best viewed in color)

B. Proposed method

In this section, the proposed SiamAPN++ is introduced in detail. As shown in Fig. 2, SiamAPN++ consists of four subnetworks, respectively the feature extraction network, APN-DF, AAN, and classification & regression network.

1) *Feature extraction network*: For fulfilling the practical requirement onboard the embedded platform, the Alexnet is chosen as the backbone of the SiamAPN++ tracker to extract effective feature maps. The feature maps from the last two layers are utilized to generate adaptive anchors. For clarification, the input template image is denoted as z , the search image is denoted as x , and the $\varphi_k(x)$ represents the search branch output of the k -th layer.

2) *Anchor proposal network*: For the sake of boosting the robustness of proposing anchors, the dual features from the feature extraction network are adopted to handling objects with various scales. Generally, the high-level features are interest in large-scale objects while the low focus on small objects. Therefore, an effective and efficient APN structure is designed to discover the internal relationship between different layers and then merely generate anchors at one. It avoids the extra computation brought by generating anchors for each feature.

Specifically, the $\varphi_4(x)$ and $\varphi_4(z)$ is used to produce the similarity map as:

$$R_4 = \mathcal{F}(\varphi_4(x) \star \varphi_4(z)) , \quad (1)$$

where the \star represents the depth-wise cross-correlation layer introduced in [8] and \mathcal{F} denotes the convolutional operation for decreasing the number of channels. Similarly, the similarity of the fifth layer is acquired as:

$$R_5 = \mathcal{F}(\varphi_5(x)) \star \mathcal{F}(\varphi_5(z)) . \quad (2)$$

Two cross-branches are designed to discover the internal relationship between R_4 and R_5 . To maintains the similarity of cross-interdependencies, the cross-AAN is utilized in the APN-DF, which is explained detailedly in AAN. After obtaining the R_A , the anchors can be calculated through two convolutional operations.

Remark 1: Since the dual feature structure exploits and integrates the preponderance of different-level features, the robustness and anti-interference ability to track objects with various scales are raised. Besides, it can also provide comprehensive position semantic information of anchors for AAN.

3) *Attentional aggregation network*: In order to promote the expression ability of feature maps and further improve the tracking performance, the AAN is designed by introducing the attentional mechanism. It can be separated into self-AAN and cross-AAN. Next, the process of adaptively enhancing self-semantic interdependencies and aggregate cross-interdependencies is elaborated.

Self-AAN: The self-AAN aims to enhance the self-semantic information of the single feature map via spatial and channel attention. The spatial attention is inspired by [22]. To explore different semantic information and avoid the influence on APN-DF, R^a is calculated as the same as R_5 . Then, by three different convolution layers, three new feature maps can be generated denoted as $\{R^q, R^k, R^v\} \in \mathbb{R}^{C \times H \times W}$. By reshaping R^q and R^k to $\mathbb{R}^{C \times (H \times W)}$, cooperating matrix multiplication, and softmax layer, the spatial attention map $R^s \in \mathbb{R}^{(H \times W) \times (H \times W)}$ can be calculated. Therefore, the output of spatial attention $R^s \in \mathbb{R}^{C \times H \times W}$ can be obtained as:

$$R_{j,i}^s = R_{j,i}^v R_{j,i}^a + R_{j,i}^a , \quad (3)$$

where i, j represents the point in (i, j) on feature map.

Since different channels of the same feature are associated with other channels, by introducing the channel attention, the semantic information can be exploited included in interdependencies between channels. It can emphasize the interdependent channels and improve the expression ability of specific semantics. To obtain exhaustive channel enhancement, the global max-pooling (GMP) and global average pooling (GAP) are adopted before FFN. Besides, the channel attention FFN is share-weight to explore the interdependencies between channels more effectively. Therefore, the calculation process of $R_c \in \mathbb{R}^{C \times H \times W}$ is as follows:

$$R_c = R^s + \gamma_1 * \text{FFN}(\text{GAP}(R^s)) * R^s + \gamma_2 * \text{FFN}(\text{GMP}(R^s)) * R^s , \quad (4)$$

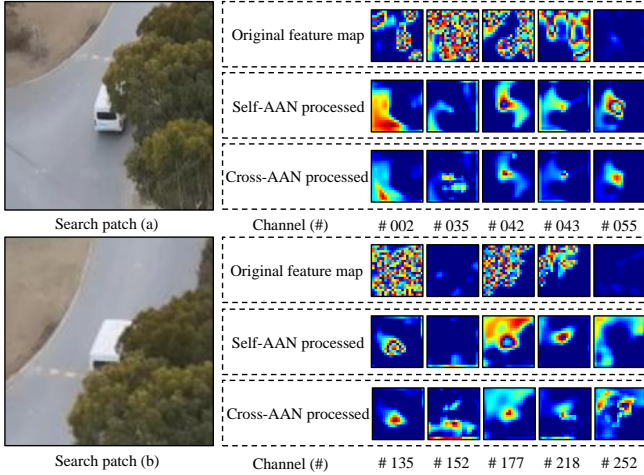


Fig. 3. Visualization of the AAN output feature maps in the real-world test. It shows that AAN indeed provides effective and robust feature maps for tracking occluded objects accurately.

where γ_k , $k = \{1, 2, 3, 4\}$ gradually learn a weight from 0 to maintain adaptively a balance between the different branches.

Remark 2: By building the spatial and channel attention, the self-AAN can aggregate and model the self-semantic interdependencies of the single feature map. Therefore, it can provide stable and robust self-attentional features for aggregating different feature maps further.

Cross-AAN: Since the anchors are generated adaptively, the semantic information about anchors is acquired for SiamAPN++ to perceive the existence of anchors. Therefore, the location information of anchors is quite significant for classification and regression performance. To aggregate the cross-interdependencies between different features and integrate the location information of anchors, cross-AAN is introduced. Based on the final feature maps, SiamAPN++ can achieve robust classification and regression results.

There are two cross paths in cross-AAN. One path applies a feedforward neural network (FFN) structure to generate a corresponding weight for each channel of R_c , aggregating the interdependencies between channels explicitly. Besides, before the FFN, GAP is cooperated to compress the feature to one dimension. The other path aims to emphasize the interdependent channels of R_A and R_c implicitly via element-wise concatenation. Therefore, the final feature maps $R \in \mathbb{R}^{C \times H \times W}$ can be computed by:

$$R = R_c + \gamma_3 * \text{FFN}(\text{GAP}(R_A)) * R_c + \gamma_4 * \mathcal{F}(\text{Cat}(R_A, R_c)) . \quad (5)$$

Remark 3: By virtue of cross-ANN, the cross-interdependencies between different feature maps are aggregated including the location information of anchors. Figure 3 clearly shows that AAN highlights adaptively the effective information from complex feature maps and effectively weakens the interference factors caused by occlusion. Eventually, based on the improved feature maps, the robustness and accuracy of SiamAPN++ are raised significantly.

4) *Classification and regression network:* The classification and regression network applies a similar structure com-

pared with the baseline SiamAPN. The multi-classification structure is also adopted. The first branch aims to classify the anchor with a high intersection over union (IoU) score. The second branch concentrates on selecting the points on the feature map that fall in ground truth areas. The last branch considers the center distance between each point and ground truth center point inspired by [12]. w_1 , w_2 , and w_3 are introduced for balancing different branches. For improving the performance of convergence, the loss function of regression is redesigned as:

$$L_{ious} = -(1 - ious) * (\alpha - ious) * \log(ious) , \quad (6)$$

where α is a hyper-parameter, reflecting the tendentiousness to positive and negative samples while $ious$ represents the IoU score between the proposed anchors and ground truth bounding box. α is set in the range of 1 to 2. It aims to increase gradient at high loss position to accelerate the convergence process, and decrease gradient at low loss position to raise the convergence accuracy. In this way, the model obtains accurate and robust convergence results faster (epoch=25) compared with the baseline (epoch=37).

IV. EVALUATIONS

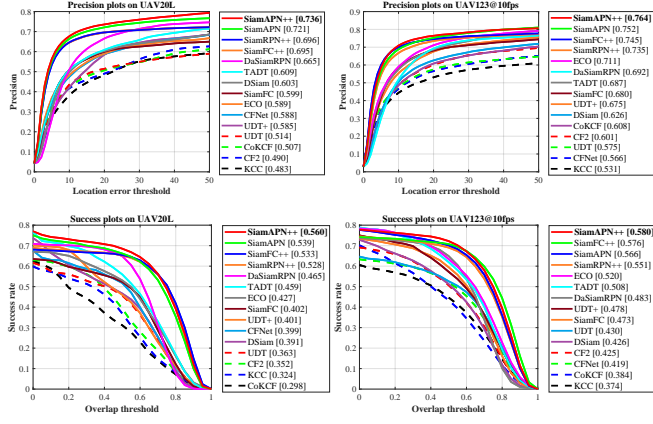
In this section, SiamAPN++ is comprehensively evaluated on two well-known authoritative UAV tracking benchmarks, *i.e.*, UAV20L [24] and UAV123@10fps [24]. Other 14 SOTA trackers are also included in the evaluation, *i.e.*, SiamAPN (baseline) [20], SiamRPN++ [8], DaSiamRPN [9], SiamFC++ [11], SiamFC [6], UDT [25], UDT+ [25], TADT [26], DSiam [27], CoKCF [28], CF2 [29], CFNet [30], ECO [31], and KCC [32].

Remark 4: To better compare the performance of different tracking strategies, all Siamese-based trackers adopt the same backbone, *i.e.*, AlexNet [33] pre-trained on ImageNet [34].

A. Implementation details

In the training process, the last three layers of the backbone are fine-tuned with a learning rate of 5×10^{-4} at first. The whole tracker are trained on the images extracted from COCO [35], ImageNet VID [34], GOT-10K [36] and Youtube-BB [37]. The stochastic gradient descent (SGD) with a minibatch of 220 pairs is applied. Besides, the momentum is set to 0.9 and weight decay is set to 10^{-4} . Following the baseline, the input size of the template image and search image are set to 127×127 pixels and 287×287 pixels. The tracking code is available at <https://github.com/vision4robotics/SiamAPN>.

The training process of the proposed method SiamAPN++ is implemented in Python using Pytorch on a PC with an Intel i9-9920X CPU, a 32GB RAM, and an NVIDIA TITAN RTX GPU. For testing the feasibility and performance of SiamAPN++ on UAV tracking, an NVIDIA Jetson AGX Xavier is adopted as the real-world tests platform. Real-world tests prove the accuracy and robustness of SiamAPN++ with a speed of around 35 frames per second (FPS) without TensorRT acceleration.



(a) Results on UAV20L

(b) Results on UAV123@10fps

Fig. 4. Overall performance of all trackers on (a) UAV20L, (b) UAV123@10fps. The overall results illustrate that SiamAPN++ achieves superior performance against other SOTA trackers.

TABLE I

AVERAGE ATTRIBUTE-BASED EVALUATION OF THE SIAMAPN++ AND OTHER 14 SOTA TRACKERS ON TWO BENCHMARKS. THE BEST THREE PERFORMANCES ARE RESPECTIVELY HIGHLIGHTED WITH **RED**, **GREEN**, AND **BLUE** COLOR.

Trackers	CM		FM		FOC		POC		SV	
	Prec.	Succ.								
ECO	0.630	0.457	0.542	0.344	0.457	0.254	0.598	0.427	0.621	0.453
SiamFC	0.626	0.432	0.529	0.319	0.487	0.264	0.577	0.385	0.614	0.416
UDT	0.512	0.375	0.470	0.303	0.413	0.226	0.493	0.350	0.513	0.375
UDT+	0.598	0.424	0.521	0.322	0.469	0.259	0.581	0.403	0.599	0.418
CF2	0.519	0.374	0.384	0.246	0.431	0.233	0.499	0.346	0.507	0.364
CFNet	0.533	0.382	0.435	0.244	0.407	0.214	0.527	0.365	0.542	0.386
CoKCF	0.525	0.329	0.414	0.210	0.418	0.205	0.512	0.309	0.520	0.311
DSiam	0.613	0.404	0.536	0.309	0.547	0.301	0.579	0.371	0.585	0.387
TADT	0.638	0.474	0.597	0.386	0.486	0.281	0.612	0.444	0.618	0.461
KCC	0.458	0.320	0.348	0.206	0.339	0.172	0.457	0.300	0.467	0.320
DaSiamRPN	0.667	0.470	0.571	0.365	0.505	0.274	0.625	0.427	0.656	0.459
SiamFC++	0.709	0.544	0.622	0.454	0.469	0.292	0.669	0.497	0.700	0.540
SiamRPN++	0.706	0.530	0.624	0.442	0.475	0.284	0.655	0.480	0.691	0.521
SiamAPN	0.721	0.537	0.710	0.493	0.520	0.308	0.680	0.493	0.715	0.537
SiamAPN++	0.742	0.564	0.711	0.507	0.577	0.358	0.702	0.519	0.729	0.554

B. Evaluation metrics

The one-pass evaluation (OPE) metrics [38] are adopted, *i.e.*, precision and success rate. Specifically, the success rate is measured as the IoU score. Besides, the success plot reflects the percentage of the frames whose IoU score beyond a pre-defined threshold and the area under the curve (AUC) of success plot is used to rank all the trackers. The precision plot shows the percentage of frames whose center location error (CLE) between the estimated bounding box and ground truth is smaller than thresholds. Note that the score at 20 pixels is utilized for ranking.

C. Evaluation on UAV benchmarks

1) *Overall performance*: The proposed method achieves an impressive improvement compared with other SOTA trackers on two well-known benchmarks.

UAV20L: UAV20L [24] contains 20 long-term sequences whose maximum sequence contains 5527 frames with an average of 2934 frames per sequence. Therefore, UAV20L is adopted for proving the long-term tracking scenes most commonly in UAV tracking. As illustrated in Fig. 4, SiamAPN++ outperforms other trackers with an improvement of **2.0%** on

TABLE II
PRECISION COMPARISON OF OUR TRACKER WITH DIFFERENT COMPONENTS ON UAV20L. NOTE THAT ARC REPRESENTS THE ASPECT RATIO CHANGE AND OC INCLUDES FULL OCCLUSION AS WELL AS PARTIAL OCCLUSION.

Structure	Overall	SV	ARC	CM	OC
Baseline	0.721	0.707	0.652	0.707	0.617
Baseline+APN-DF	0.727	0.715	0.662	0.713	0.649
Baseline+APN-DF+self-AAN	0.730	0.716	0.663	0.716	0.647
Baseline+APN-DF+AAN	0.736	0.722	0.670	0.722	0.651

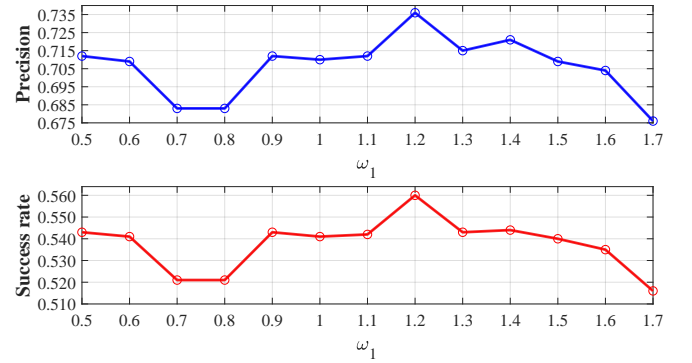


Fig. 5. Key parameter analysis of w_1 on UAV20L. When the $w_1 = 1.2$, SiamAPN++ achieves the best overall performance.

precision and **4.0%** on AUC score comparing to the second-best tracker.

UAV123@10fps: UAV123@10fps [24] contains 123 sequences with a frame-rate of 10 FPS. Since the frame interval becomes larger than 30 FPS, the movement and variation of the object become more drastic, bringing difficulties to the tracking task. Therefore, UAV123@10fps [24] is chosen to comprehensively evaluate the robustness under severe variation. Overall performance shown in Fig. 4 proves the superior robustness and accuracy of SiamAPN++ in precision (0.764) and AUC score (0.580).



Fig. 6. Screenshots of *person7_2*, *car11* from UAV123@10fps, and *person19* from UAV20L. The tracking videos can be found here: <https://youtu.be/okS289p3pCQ>.

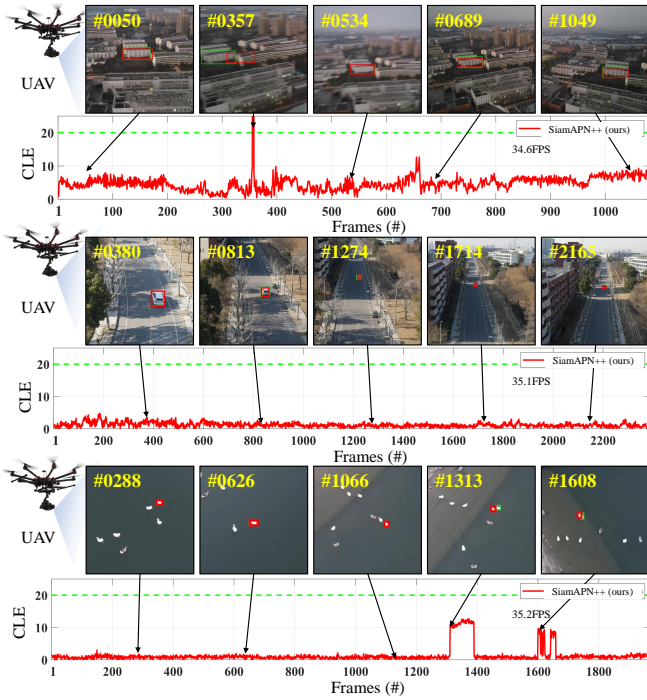


Fig. 7. Real-world tests in terms of CLE onboard the embedded platform. The tracking objects from the top to bottom are building, car, and duck. Besides, the tracking results and ground truth are marked with red and green box. The CLE score below the green dotted line is considered as the effective tracking result.

2) *Attribute-based performance*: To analyze the robustness of SiamAPN++ under various challenges, the average attribute-based evaluation results on two UAV benchmarks are shown in TABLE I. There are five most common attributes in UAV tracking challenges are analyzed, *i.e.*, camera motion (CM), fast motion (FM), full occlusion (FOC), partial occlusion (POC), and scale variation (SV). Attributing to the AAN and dual feature structure, SiamAPN++ achieves impressive performance in the CM scenarios with a **5.0%** promotion on AUC score. Besides, our tracker surpasses the baseline in terms of FM. Meantime, in the FOC conditions, SiamAPN++ exceeds the second-best tracker with a huge improvement of **5.5%** in precision and **16.2%** in AUC score.

3) *Ablation study*: To demonstrate the effectiveness of the APN-DF and AAN, the precision of SiamAPN++ with different components and the baseline SiamAPN on UAV20L is listed in TABLE II. With the internal relationship introduced by the APN-DF, the tracker has surpassed the baseline. Besides, it indeed promotes performance when tracking objects with various scales. Furthermore, attributing to the AAN, the self-interdependencies from the single feature map and the cross-interdependencies are aggregated, further improving the accuracy of SiamAPN++.

4) *Key parameter analysis*: Since the first classification branch, *i.e.*, w_1 , directly reflects the classification tendentiousness to anchors, w_1 has important influence in tracking performance. Obviously, too large w_1 will influence the effectiveness of other branches, while too small w_1 will impede the promotion introduced by anchor information on classification. Therefore, to evaluate the influence of w_1 , w_1

is set to different values for further research. It is set from 0.5 and increases in a small step of 0.1. As presented in Fig. 5, the AUC and precision of SiamAPN++ achieve best performance when $w_1 = 1.2$. Please note that w_1 is set to 1.2 during the evaluation above and the real-world tests.

5) *Qualitative Evaluation*: Some qualitative comparisons are shown in Fig. 6. The main challenges of these sequences include SV, ARC, FM, POC, CM, and out-of-view. By the combination of APN-DF and AAN, SiamAPN++ achieves superior tracking performance eventually.

V. REAL-WORLD TESTS

To verify the feasibility of the proposed tracker, real-world tests are conducted onboard the embedded platform. Four real-world test results are presented in this paper includes car, building, and duck.

The main challenges in the first test are severe CM, POC, and similar objects. Although there are some errors due to the blurring caused by severe CM, SiamAPN++ can determine the location of the object again and achieve impressive long-term tracking performance. By aggregating self and cross-interdependencies between feature maps, SiamAPN++ can handle the LR, SV, ARC challenges effectively, thereby tracking the car accurately and robustly. The robustness of SiamAPN++ is significantly increased via exploiting the location information of anchors. Based on it, the AAN can explore the effective interdependencies between feature maps, achieve impressive tracking performance in the third test. The fifth test mainly focuses on the occluded object. Figure 1 illustrates the combination of AAN and APN-DF indeed assist to determine the location of the object again.

During the real-world tests, our tracker maintains robust and accurate performance with an average speed of 34.9 FPS. In a word, the real-world tests strongly prove the superior performance of SiamAPN++ under various challenges with a promising speed in UAV tracking.

VI. CONCLUSION

In this work, a novel attentional Siamese-based tracker is introduced for fulfilling the performance and feasibility requirement of real-time UAV tracking. The self-AAN is proposed for aggregating the self-interdependencies of the single feature. Besides, to aggregate the cross-interdependencies between different feature maps, we also propose the cross-AAN. In addition, the dual feature structure integrates different feature maps effectively. In the end, real-world tests strongly verify the practicability of our tracker. Consequently, we are convinced that our work can boost the development of UAV tracking-related applications.

ACKNOWLEDGMENT

This work is supported by the National Natural Science Foundation of China (No. 61806148) and the Natural Science Foundation of Shanghai (No. 20ZR1460100).

REFERENCES

[1] R. Bonatti, C. Ho, W. Wang, S. Choudhury, and S. Scherer, "Towards a Robust Aerial Cinematography Platform: Localizing and Tracking Moving Targets in Unstructured Environments," in *Proceedings of the IEEE/RSJ International Conference on Intelligent Robots and Systems (IROS)*, 2019, pp. 229–236.

[2] G. J. Laguna and S. Bhattacharya, "Path planning with Incremental Roadmap Update for Visibility-based Target Tracking," in *Proceedings of the IEEE/RSJ International Conference on Intelligent Robots and Systems (IROS)*, 2019, pp. 1159–1164.

[3] H. Cheng, L. Lin, Z. Zheng, Y. Guan, and Z. Liu, "An Autonomous Vision-Based Target Tracking System for Rotorcraft Unmanned Aerial Vehicles," in *Proceedings of the IEEE/RSJ International Conference on Intelligent Robots and Systems (IROS)*, 2017, pp. 1732–1738.

[4] Z. Huang, C. Fu, Y. Li, F. Lin, and P. Lu, "Learning Aberrance Repressed Correlation Filters for Real-time UAV Tracking," in *Proceedings of the IEEE International Conference on Computer Vision (ICCV)*, 2019, pp. 2891–2900.

[5] Y. Li, C. Fu, F. Ding, Z. Huang, and G. Lu, "AutoTrack: Towards High-Performance Visual Tracking for UAV With Automatic Spatio-Temporal Regularization," in *Proceedings of the IEEE/CVF Conference on Computer Vision and Pattern Recognition (CVPR)*, 2020, pp. 11920–11929.

[6] L. Bertinetto, J. Valmadre, J. F. Henriques, A. Vedaldi, and P. H. Torr, "Fully-Convolutional Siamese Networks for Object Tracking," in *Proceedings of the European Conference on Computer Vision (ECCV)*, 2016, pp. 850–865.

[7] B. Li, J. Yan, W. Wu, Z. Zhu, and X. Hu, "High Performance Visual Tracking with Siamese Region Proposal Network," in *Proceedings of the IEEE/CVF Conference on Computer Vision and Pattern Recognition (CVPR)*, 2018, pp. 8971–8980.

[8] B. Li, W. Wu, Q. Wang, F. Zhang, J. Xing, and J. Yan, "SiamRPN++: Evolution of Siamese Visual Tracking With Very Deep Networks," in *Proceedings of the IEEE/CVF Conference on Computer Vision and Pattern Recognition (CVPR)*, 2019, pp. 4277–4286.

[9] Z. Zhu, Q. Wang, B. Li, W. Wu, J. Yan, and W. Hu, "Distractor-Aware Siamese Networks for Visual Object Tracking," in *Proceedings of the European Conference on Computer Vision (ECCV)*, 2018, pp. 101–117.

[10] Y. Yu, Y. Xiong, W. Huang, and M. R. Scott, "Deformable Siamese Attention Networks for Visual Object Tracking," in *Proceedings of the IEEE/CVF Conference on Computer Vision and Pattern Recognition (CVPR)*, 2020, pp. 6727–6736.

[11] Y. Xu, Z. Wang, Z. Li, Y. Yuan, and G. Yu, "SiamFC++: Towards Robust and Accurate Visual Tracking with Target Estimation Guidelines," in *Proceedings of the AAAI Conference on Artificial Intelligence (AAAI)*, 2020, pp. 12549–12556.

[12] D. Guo, J. Wang, Y. Cui, Z. Wang, and S. Chen, "SiamCAR: Siamese Fully Convolutional Classification and Regression for Visual Tracking," in *Proceedings of the IEEE/CVF Conference on Computer Vision and Pattern Recognition (CVPR)*, 2020, pp. 6268–6276.

[13] Q. Wang, Z. Teng, J. Xing, J. Gao, W. Hu, and S. Maybank, "Learning Attentions: Residual Attentional Siamese Network for High Performance Online Visual Tracking," in *Proceedings of the IEEE/CVF Conference on Computer Vision and Pattern Recognition (CVPR)*, 2018, pp. 4854–4863.

[14] D. S. Bolme, J. R. Beveridge, B. A. Draper, and Y. M. Lui, "Visual Object Tracking Using Adaptive Correlation Filters," in *Proceedings of the IEEE/CVF Conference on Computer Vision and Pattern Recognition (CVPR)*, 2010, pp. 2544–2550.

[15] H. K. Galoogahi, A. Fagg, and S. Lucey, "Learning Background-Aware Correlation Filters for Visual Tracking," in *Proceedings of the IEEE International Conference on Computer Vision (ICCV)*, 2017, pp. 1144–1152.

[16] C. Fu, J. Ye, J. Xu, Y. He, and F. Lin, "Disruptor-Aware Interval-Based Response Inconsistency for Correlation Filters in Real-Time Aerial Tracking," *IEEE Transactions on Geoscience and Remote Sensing*, pp. 1–13, 2020.

[17] R. Tao, E. Gavves, and A. W. M. Smeulders, "Siamese Instance Search for Tracking," in *Proceedings of the IEEE/CVF Conference on Computer Vision and Pattern Recognition (CVPR)*, 2016, pp. 1420–1429.

[18] B. Li, J. Yan, W. Wu, Z. Zhu, and X. Hu, "High Performance Visual Tracking with Siamese Region Proposal Network," in *Proceedings of the IEEE/CVF Conference on Computer Vision and Pattern Recognition (CVPR)*, 2018, pp. 8971–8980.

[19] Z. Zhang and H. Peng, "Deeper and Wider Siamese Networks for Real-Time Visual Tracking," in *Proceedings of the IEEE/CVF Conference on Computer Vision and Pattern Recognition (CVPR)*, 2019, pp. 4586–4595.

[20] C. Fu, Z. Cao, Y. Li, J. Ye, and C. Feng, "Siamese Anchor Proposal Network for High-Speed Aerial Tracking," in *Proceedings of the IEEE International Conference on Robotics and Automation (ICRA)*, 2021, pp. 1–7.

[21] X. Wang, R. Girshick, A. Gupta, and K. He, "Non-local Neural Networks," in *Proceedings of the IEEE/CVF Conference on Computer Vision and Pattern Recognition (CVPR)*, 2018, pp. 7794–7803.

[22] J. Fu, J. Liu, H. Tian, Y. Li, Y. Bao, Z. Fang, and H. Lu, "Dual Attention Network for Scene Segmentation," in *Proceedings of the IEEE/CVF Conference on Computer Vision and Pattern Recognition (CVPR)*, 2019, pp. 3141–3149.

[23] Q. Wang, B. Wu, P. Zhu, P. Li, W. Zuo, and Q. Hu, "ECA-Net: Efficient Channel Attention for Deep Convolutional Neural Networks," in *Proceedings of the IEEE/CVF Conference on Computer Vision and Pattern Recognition (CVPR)*, 2020, pp. 11531–11539.

[24] M. Mueller, N. Smith, and B. Ghanem, "A Benchmark and Simulator for UAV Tracking," in *Proceedings of the European Conference on Computer Vision (ECCV)*, 2016, pp. 445–461.

[25] N. Wang, Y. Song, C. Ma, W. Zhou, W. Liu, and H. Li, "Unsupervised Deep Tracking," in *Proceedings of the IEEE/CVF Conference on Computer Vision and Pattern Recognition (CVPR)*, 2019, pp. 1308–1317.

[26] X. Li, C. Ma, B. Wu, Z. He, and M. Yang, "Target-Aware Deep Tracking," in *Proceedings of the IEEE/CVF Conference on Computer Vision and Pattern Recognition (CVPR)*, 2019, pp. 1369–1378.

[27] Q. Guo, W. Feng, C. Zhou, R. Huang, L. Wan, and S. Wang, "Learning Dynamic Siamese Network for Visual Object Tracking," in *Proceedings of the IEEE International Conference on Computer Vision (ICCV)*, 2017, pp. 1781–1789.

[28] L. Zhang and P. N. Suganthan, "Robust Visual Tracking via Co-Trained Kernelized Correlation Filters," *Pattern Recognition*, vol. 69, pp. 82–93, 2017.

[29] C. Ma, J. Huang, X. Yang, and M. Yang, "Hierarchical Convolutional Features for Visual Tracking," in *Proceedings of the IEEE International Conference on Computer Vision (ICCV)*, 2015, pp. 3074–3082.

[30] J. Valmadre, L. Bertinetto, J. Henriques, A. Vedaldi, and P. H. S. Torr, "End-to-End Representation Learning for Correlation Filter Based Tracking," in *Proceedings of the IEEE Conference on Computer Vision and Pattern Recognition (CVPR)*, 2017, pp. 5000–5008.

[31] M. Danelljan, G. Bhat, F. S. Khan, and M. Felsberg, "ECO: Efficient Convolution Operators for Tracking," in *Proceedings of IEEE Conference on Computer Vision and Pattern Recognition (CVPR)*, 2017, pp. 6931–6939.

[32] C. Wang, L. Zhang, L. Xie, and J. Yuan, "Kernel Cross-Correlator," in *Proceedings of the AAAI Conference on Artificial Intelligence (AAAI)*, vol. 32, no. 1, 2018, pp. 4179–4186.

[33] A. Krizhevsky, I. Sutskever, and G. E. Hinton, "Imagenet Classification with Deep Convolutional Neural Networks," in *Advances in neural information processing systems (NIPS)*, 2012, pp. 1097–1105.

[34] O. Russakovsky, J. Deng, H. Su, J. Krause, S. Satheesh, S. Ma, Z. Huang, A. Karpathy, A. Khosla, M. Bernstein, et al., "Imagenet Large Scale Visual Recognition Challenge," *International Journal of Computer Vision*, vol. 115, no. 3, pp. 211–252, 2015.

[35] T.-Y. Lin, M. Maire, S. Belongie, J. Hays, P. Perona, D. Ramanan, P. Dollár, and C. L. Zitnick, "Microsoft coco: Common objects in context," in *Proceedings of the European conference on computer vision (ECCV)*, 2014, pp. 740–755.

[36] L. Huang, X. Zhao, and K. Huang, "GOT-10k: A Large High-Diversity Benchmark for Generic Object Tracking in the Wild," *IEEE Transactions on Pattern Analysis and Machine Intelligence*, pp. 1–17, 2019.

[37] E. Real, J. Shlens, S. Mazzocchi, X. Pan, and V. Vanhoucke, "YouTube-BoundingBoxes: A Large High-Precision Human-Annotated Data Set for Object Detection in Video," in *Proceedings of the IEEE/CVF Conference on Computer Vision and Pattern Recognition (CVPR)*, 2017, pp. 7464–7473.

[38] Y. Wu, J. Lim, and M. Yang, "Online Object Tracking: A Benchmark," in *Proceedings of the IEEE Conference on Computer Vision and Pattern Recognition*, 2013, pp. 2411–2418.